Title

Fungus-like mycelial fossils in 2.4-billion-year-old vesicular basalt

Journal

Nature Ecology & Evolution, 1(6)

ISSN

2397-334X

Authors

Bengtson, Stefan
Rasmussen, Birger
Ivarsson, Magnus
et al.

Publication Date

2017

DOI

10.1038/s41559-017-0141

Peer reviewed

REPORT

GEOCHEMISTRY

Titanium isotopic evidence for felsic crust and plate tectonics 3.5 billion years ago

Nicolas D. Greber,[1]*† Nicolas Dauphas,[1] Andrey Bekker,[2,3] Matouš P. Ptáček,[1] Ilya N. Bindeman,[4] Axel Hofmann[3]

Earth exhibits a dichotomy in elevation and chemical composition between the continents and ocean floor. Reconstructing when this dichotomy arose is important for understanding when plate tectonics started and how the supply of nutrients to the oceans changed through time. We measured the titanium isotopic composition of shales to constrain the chemical composition of the continental crust exposed to weathering and found that shales of all ages have a uniform isotopic composition. This can only be explained if the emerged crust was predominantly felsic (silica-rich) since 3.5 billion years ago, requiring an early initiation of plate tectonics. We also observed a change in the abundance of biologically important nutrients phosphorus and nickel across the Archean-Proterozoic boundary, which might have helped trigger the rise in atmospheric oxygen.

Modern oceanic crust, produced by mantle melting, is basaltic in composition and is continuously recycled into the mantle at subduction zones. Earth's earliest crust was also presumably mafic but eventually evolved into two distinct components: an oceanic crust composed of mafic minerals (dark-colored; rich in magnesium and iron) and a continental crust bearing felsic minerals (light-colored; rich in silicon and aluminum). Constraining when a felsic crust first developed and how its chemical composition changed through time are important questions because the composition of the crust influences the composition of the atmosphere, controls the flux of biologically important nutrients to the ocean, and is related to the initiation of plate tectonics (*1*–*4*). This issue has been, however, the subject of much controversy (*4*–*12*), reflecting the difficulty in interpreting Earth's earliest rock record. To reconstruct the chemical composition of the continental crust through time, many studies have relied on chemical analyses of fine-grained, terrigenous sediments (shales) (*5*, *9*, *10*). Shales are the product of physical and chemical weathering of the part of the crust that is above sea level and exposed to the atmosphere (hereafter referred to as "emerged crust"). Using the chemical composition of shales as a proxy for the emerged crust is challenging because their composition can be modified by weathering, grain size sorting during transport, and sediment diagenesis (*5*). As a result, aspects of the shale composition observed today—such as their silica (SiO_2) content—might no longer reflect those of their source rocks.

We developed a proxy for reconstructing the chemical composition of the emerged crust based on analyses of the titanium (Ti) isotopic composition of shales. This proxy is based on the observation that in igneous rocks, the $^{49}Ti/^{47}Ti$ ratio (expressed as $\delta^{49}Ti$; the deviation in parts per thousand of the $^{49}Ti/^{47}Ti$ ratio relative to the Origins Laboratory Ti reference material) correlates with the SiO_2 concentration (Fig. 1 and table S1). This is most likely the result of preferential incorporation of light Ti isotopes into Fe-Ti oxides during fractional crystallization (*13*). Mid-ocean ridge, island arc, and ocean island basalts, as well as komatiites, have within error the same $\delta^{49}Ti$ value as the bulk silicate Earth [+0.005 ± 0.005 per mil (‰); 95% confidence interval (CI)] (*13*, *14*). More evolved rocks of Phanerozoic and Archean ages have heavier $\delta^{49}Ti$ values that reach +0.6 ‰ at a SiO_2 concentration of 75 weight % (wt %) (Fig. 1). Therefore, by measuring the $\delta^{49}Ti$ value of shales, the SiO_2 content of their source rocks can be estimated, providing constraints on the proportion of mafic and felsic rocks in the emerged continental crust. This system overcomes several important shortcomings of previous studies: (i) Ti is highly insoluble in terrestrial surface environments (*15*), so its isotopic composition is immune to processes involving water-rock interactions such as weathering and diagenesis. (ii) On Earth, Ti is present under a single oxidation state (Ti^{4+}), so its chemical behavior is not affected by fluctuating redox conditions in the atmosphere and oceans. (iii) Ti is biologically inert and was thus not affected by the large-scale biogeochemical reorganizations that affected terrestrial surface environments. (iv) During weathering, Ti is incorporated into clay and silt fractions (*16*, *17*), so that Ti in shales is minimally affected by grain size sorting during riverine and oceanic transport (*18*).

We measured the $\delta^{49}Ti$ values of 48 individual shale samples (table S2), as well as 30 composite samples, which are mixtures of several shale samples with similar ages and locations (table S3) (*18*). At any given age, some scatter is noticeable in the $\delta^{49}Ti$ value, indicating that local source rocks influenced the Ti isotopic composition of the shale. A similar feature has also been observed in the neodymium (Nd) isotopic composition of shales (*19*). Nevertheless, the average $\delta^{49}Ti$ value of shales is almost constant over the past 3.5 billion years, exhibiting only a subtle shift toward heavier values from the Archean to the present (Fig. 2). The average shale $\delta^{49}Ti$ value is always heavier than that of basalts and komatiites (Fig. 2), indicating that felsic rocks were the major constituent of the emerged crust throughout the past 3.5 billion years.

The chemical composition of shales is the result of the erosion of diverse rock types present in the crust. Some of these rocks have very different Ti concentrations (for example, ~0.95 and ~0.25 wt % TiO_2 for typical basalts and granites, respectively), so that shale $\delta^{49}Ti$ values are more heavily influenced by basaltic than granitic input. We have developed a mixing model to translate the $\delta^{49}Ti$ values of shales into an estimate of the crustal composition, assuming that the emerged continental crust is composed of three end-member rock types. These correspond to mafic (M; SiO_2 = 45 to 52 wt %, MgO <18 wt %), felsic (F; SiO_2 = 63 to 80 wt %), and komatiitic (K; Archean komatiites with MgO >18 wt %) rocks. A complication to this mixing model is that magma compositions changed through time, reflecting the secular cooling of Earth and the transfer of incompatible elements into Earth's crust (*20*–*22*). Furthermore, ultramafic komatiitic magmas were common in the Archean, whereas they almost disappeared after ~2.4 billion years ago (Ga) (*23*, *24*). The chemical compositions of the end-members relevant to Earth's early history therefore differ slightly from those of their more recent counterparts. Hence, following (*20*), we assume that the transition from Archean-type to modern-type mafic and felsic end-members occurred gradually across the Archean-Proterozoic boundary (tables S4 and S5) (*18*).

A three-component mixture cannot be resolved by relying solely on the $\delta^{49}Ti$ value of shales. In particular, the $\delta^{49}Ti$ values of komatiites are identical to those of mafic rocks, but their Ti concentrations resemble felsic rocks. Because komatiites are strongly enriched in nickel (Ni) relative to cobalt (Co) (Ni/Co ≈ 16) compared with either mafic or felsic rocks (Ni/Co ≈ 2 to 3), the Ni/Co ratio is a sensitive indicator of the contribution of the komatiite component to terrigenous sediments (fig. S1) (*9*). Thus, the combination of $\delta^{49}Ti$ values and Ni/Co ratios allows us to calculate the contributions of mafic, felsic, and komatiitic

[1]Origins Laboratory, Department of the Geophysical Sciences and Enrico Fermi Institute, The University of Chicago, 5734 South Ellis Avenue, Chicago, IL 60615, USA. [2]Department of Earth Sciences, University of California, Riverside, CA 92521, USA. [3]Department of Geology, University of Johannesburg, Post Office Box 524, Auckland Park, 2006, Republic of South Africa. [4]Department of Geological Sciences, 1272 University of Oregon, Eugene, OR 97403, USA.
*Corresponding author. Email: nicolas.greber@unige.ch
†Present address: Department of Earth Sciences, University of Geneva, Rue des Maraîchers 13, 1205 Geneva, Switzerland.

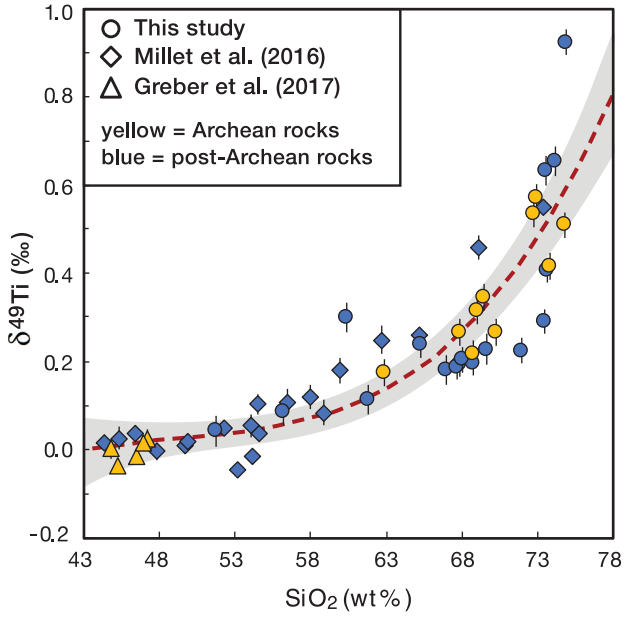

Fig. 1. Correlation between Ti isotopic composition and SiO_2 concentration in igneous rocks. Archean (yellow symbols, tonalite-trondhjemite-granodiorites and komatiites) and post-Archean (blue symbols) igneous rocks define identical correlations between SiO_2 (x) and $\delta^{49}Ti$ (y). The red dashed curve ($y = -4.132356 + 0.242697 \times x - 0.004782 \times x^2 + 3.1833 \times 10^{-5} \times x^3$) and the gray band are the polynomial fit and associated error (95% CI). Data are from (*13*, *14*) and this study.

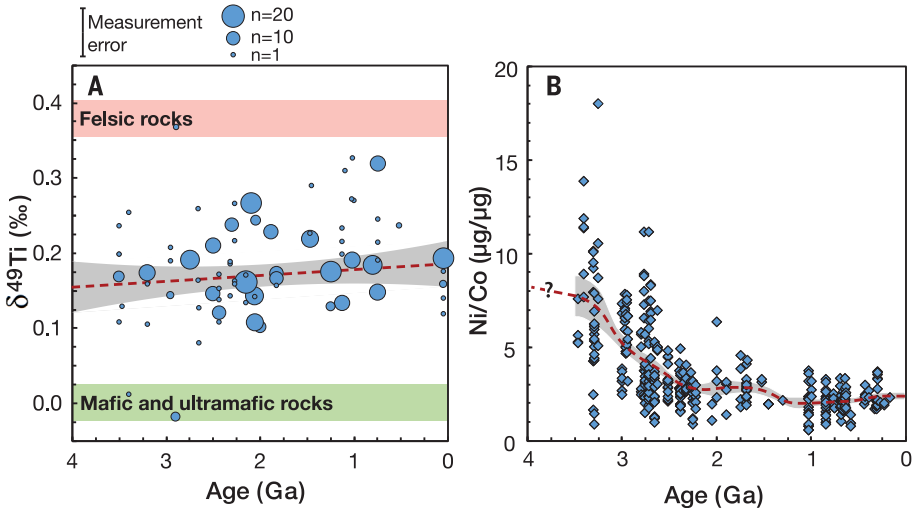

Fig. 2. Trends of Ti isotopic composition and Ni/Co ratio of terrigenous sediments through time. (**A**) Measured $\delta^{49}Ti$ values of single and composite shale samples (symbol surface area is proportional to the number of samples in the composite). The red dashed line and gray band are a linear regression through the data ($\delta^{49}Ti = -0.0077948 \times T + 0.1857$, with T being the age in billion years) and its error (95% CI). The $\delta^{49}Ti$ values of shales are always significantly heavier than those of mafic and ultramafic rocks (~0 ‰), indicating that felsic rocks contributed to a substantial fraction of terrigenous sediments since 3.5 Ga. (**B**) Ni/Co ratio of terrigenous sediments compiled from literature data (*18*). The line is a nonparametric regression through the data by using a moving average and square kernel of 0.15-billion-year width. The gray band is the 95% CI of the moving average. The higher Ni/Co ratio of Archean sediments reflects the contribution of komatiites to terrigenous sediments.

components to shales and by extension to reconstruct the composition of the emerged crust. The mass fractions of the felsic, mafic, and komatiitic components in a given shale are noted f_F, f_M, and f_K. These govern the shale composition through the following mass-balance equations:

$$\left(\frac{Ni}{Co}\right)_{shale} = \frac{f_F(Ni/Co)_F[Co]_F + f_M(Ni/Co)_M[Co]_M + f_K(Ni/Co)_K[Co]_K}{f_F[Co]_F + f_M[Co]_M + f_K[Co]_K} \quad (1)$$

$$\delta^{49}Ti_{shale} = \frac{f_F[Ti]_F\delta^{49}Ti_F + f_M[Ti]_M\delta^{49}Ti_M + f_K[Ti]_K\delta^{49}Ti_K}{f_F[Ti]_F + f_M[Ti]_M + f_K[Ti]_K} \quad (2)$$

$$1 = f_F + f_M + f_K \quad (3)$$

where [Co] and [Ti] are concentrations of the various end-members (table S4). This system of three independent equations was solved for f_F, f_M, and f_K for every time in Earth's history, based on the $\delta^{49}Ti$ values of shales and published Ni/Co ratios of terrigenous sediments (Fig. 2). Our model is insensitive to the proportion of chemical sediments such as carbonates that represent ~10% of the rocks exposed on the continental surface today (*25*). Another caveat is that shales are only sensitive to the nature of the emerged crust. Our analysis does not constrain the total volume of Earth's crust or the chemical composition of submerged crust.

Although Ti isotopes are not affected by fluid alteration, Ni is weakly soluble in aqueous media and can be fractionated by chemical weathering and postdepositional processes, such as hydrothermal alteration (*3*). Thus, it is important to ensure that the only samples considered are those that show no evidence for Ni/Co fractionation during weathering and diagenesis. To remove potentially altered samples, we filtered our database and excluded samples that fell outside the magmatic trend in Ni/Co versus chromium/scandium (Cr/Sc) ratios (fig. S2 and tables S6 and S7) (*18*). After filtering, we found a decrease in the Ni/Co ratios of terrigenous sediments from 3.5 to 2.25 Ga that then remained constant at the value found in modern sediments (Fig. 2B). This trend is consistent with the independently observed decrease in komatiite abundance at the end of the Archean (*23*, *24*).

The mixing model shows that heavy $\delta^{49}Ti$ values in shales of all ages can only be explained if felsic lithologies dominated the emerged crust since at least 3.5 Ga (Fig. 3). Although the proportion of mafic rock remained constant at ~30 ± 8 wt % throughout Earth's history, the amount of felsic rock increased from 58 ± 9 to 72 ± 8 wt %, with the major shift occurring gradually from 3.5 to 2.25 Ga (Fig. 3 and table S8). This increase coincided with the sharp decrease in komatiite abundance from 15 ± 5 wt % at 3.5 Ga to < 1 wt % at 2.25 Ga. These abundances are operative estimates because the mixing calculation does not distinguish between igneous rocks and supracrustal terrigenous sediments. In particular, we calculated that komatiites represented 15 ± 5 wt % of emerged rocks at 3.5 Ga, whereas only a few greenstone belts contain such a high proportion (*23*). These 3.5-billion-year-old shales possibly received the contribution from older supracrustal detrital sediments deposited when komatiites were more prevalent in the upper crust. Knowing the relative proportions of komatiitic, mafic, and felsic rocks, we can use the estimated end-member compositions to calculate the average composition of the emerged crust as a function of age (Fig. 3 and table S8). For example, the average SiO_2 concentration increased from 61 to 65 (±2) wt % from 3.5 Ga to the present, corresponding to an andesitic to dacitic composition (Fig. 3).

We tested the sensitivity of our model to changes in the definitions of the end-members and in assumptions on how the igneous end-members evolved through time (*18*). The reconstructed chemical compositions and rock proportions are similar in all considered scenarios (figs. S3, S4, and S5), demonstrating the robustness of our results. We also compared our calculated composition of

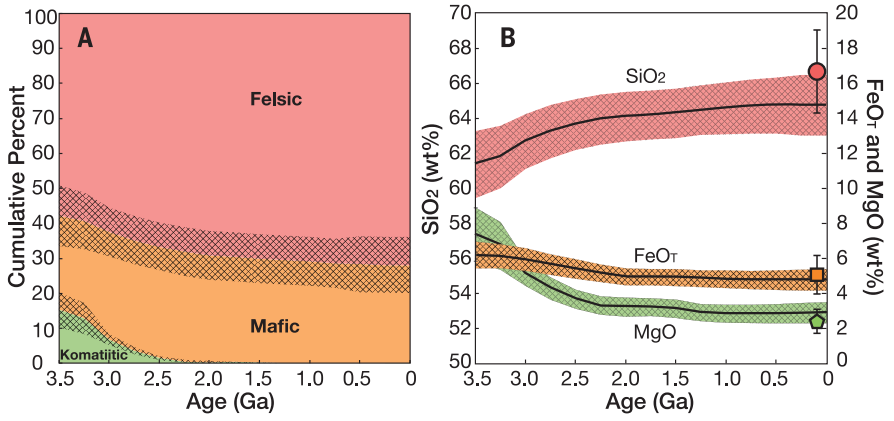

Fig. 3. Proportions of felsic, mafic, and komatiitic rocks and evolution of SiO_2, FeO_T, and MgO concentrations in Earth's emerged crust through time. (**A**) Mass proportions of rock lithologies were calculated with Eqs. 1 to 3 applied to the $\delta^{49}Ti$ and Ni/Co shale records shown in Fig. 2. The shaded areas are errors (95% CI) propagated by using a Monte Carlo approach (10,000 simulations). (**B**) Modeled average SiO_2 (left axis) and MgO and FeO_T (right axis) concentrations of the emerged crust. Modern values agree within error with the estimates from (*26*), which are shown as solid symbols.

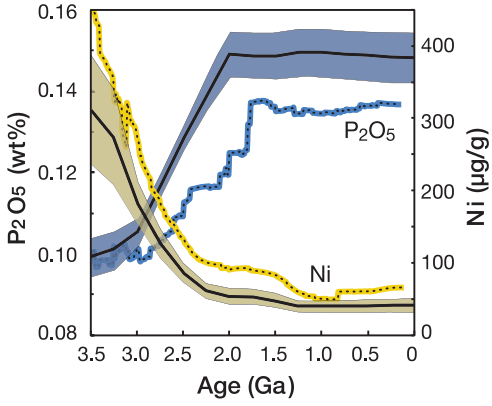

Fig. 4. Modeled evolution of Ni and P concentrations in Earth's emerged crust through time. The blue and yellow curves are the calculated P_2O_5 (left axis) and Ni (right axis) concentrations of the emerged crust, respectively. The solid curves with associated errors (95% CI) are calculated by progressively substituting both the mafic and felsic end-members across the Archean-Proterozoic boundary (*18*). The dotted lines (without errors) use all igneous rocks that are older than the age considered to define the end-member compositions (sensitivity test 4) (*18*). The higher Ni and lower P_2O_5 concentrations for the latter model are due to larger contributions of Archean rocks to the end-member compositions (*18*). Both models show an increase in P and decrease in Ni across the Archean-Proterozoic boundary, reflecting changes in the P concentration of mafic rocks (fig. S8) and the disappearance of Ni-rich komatiites (Fig. 3) at around that time.

the modern emerged crust (table S8) with an independent estimate of the upper continental crust (*26*). For the vast majority of elements, both estimates agree within error (fig. S6). Our calculated modern-day proportion of mafic to felsic rock (Fig. 3) is likewise in agreement with recent estimates based on the areal extent of modern rocks (*18*, *25*). Thus, detritus from mafic and ultramafic rocks are not strongly overrepresented in shales, even though they are less resistant to chemical weathering. Our mixing models can also explain previously documented variations in the thorium/scandium (Th/Sc) and lanthanum/scandium (La/Sc) ratios of shales (fig. S7), which were interpreted to reflect a shift in the composition of the crust from more mafic to more felsic (*5*). These shifts instead reflect changes in the composition of mafic and felsic magmas, which became progressively enriched in incompatible elements (Th and La) because of the lower degrees of partial melting that accompanied the cooling of Earth (*20*) and larger degrees of intracrustal differentiation (fig. S8 and table S4).

The Ti isotopic record of shales, combined with Ni/Co data, requires that felsic lithologies were the most abundant component of the emerged crust since at least 3.5 Ga. Our results contrast with other studies (*8*, *9*) that suggest that the upper continental crust was predominantly mafic during the Archean Eon and evolved toward a more felsic composition between 3 and 2 Ga. These studies interpreted the inferred low proportion of felsic rocks in the Early Archean as evidence that subduction-driven plate tectonics was not initiated before ~3.0 Ga. Following the same line of reasoning, we conclude that plate tectonics with subduction of oceanic crust was already in operation at 3.5 Ga and possibly even earlier. Because melting of an anhydrous basaltic source is expected to generate only low amounts of felsic magmas (*27*), an emerged crust containing almost twice as much felsic as mafic rock cannot be produced without a continuous supply of water to the melting region. Recycling of hydrated oceanic crust or oceanic plateaus at subduction zones provides such a supply in a plate tectonics regime. Felsic crust can also be generated without plate tectonics by the melting of hydrated basalts at the base of a thickened crust (*28*). The lower part of the crust is, however, generally dry (*4*). In Iceland, interaction of a mantle plume with the Mid-Atlantic ridge produces a thick crust and high geothermal gradient comparable with those inferred for the Archean (*29*, *30*), but its crust is mainly mafic and contains only 11% of felsic rock (*31*). Thus, melting at the base of a thickened mafic crust is unlikely to produce the observed high felsic-to-mafic rock ratio 3.5 Ga.

The nature of the emerged crust influenced Earth's atmospheric composition (*1*) and ocean chemistry (*25*). It also controlled the availability of biologically important nutrients in the oceans. The decrease in the abundance of komatiites between 3.5 and 2.25 Ga caused a decrease in the average Ni content of the emerged crust from 313 ± 74 µg/g in the Archean to 43 ± 10 µg/g in the post-Archean (Fig. 4). Ni is a metal cofactor in enzymes involved in microbial methanogenesis (*3*). The high Ni abundance in the emerged crust during the Archean and associated high flux of Ni to the oceans might have helped sustain a higher abundance of biogenic CH_4 in the water column and atmosphere at that time (*3*). We also found a 50% increase in the concentration of P (from 0.10 to 0.15 wt % P_2O_5) (Fig. 4) across the Archean-Proterozoic boundary, mainly driven by the higher average P_2O_5 concentration of post-Archean mafic rocks (0.19 wt %) compared with Archean mafic rocks (0.11 wt %) (fig. S8). P is one of the main limiting nutrients for biological productivity in the modern ocean (*32*). The surface area of continents exposed to weathering may have increased across the Archean-Proterozoic boundary (*1*, *2*), which would have further bolstered the export of P to the oceans (*2*). It is thus likely that biological productivity was stimulated by an increase in the supply of P at the Archean-Proterozoic transition, which might have paved the way for the expansion of oxygenic photosynthesis and the rise in atmospheric O_2 that occurred ~2.45 Ga (*33*).

REFERENCES AND NOTES

1. C.-T. A. Lee *et al.*, *Nat. Geosci.* **9**, 417–424 (2016).
2. N. Flament, N. Coltice, P. F. Rey, *Precambrian Res.* **229**, 177–188 (2013).
3. K. O. Konhauser *et al.*, *Nature* **458**, 750–753 (2009).
4. N. Arndt, *Geochem. Perspect.* **2**, 405–533 (2013).
5. S. R. Taylor, S. M. McLennan, *The Continental Crust: Its Composition and Evolution* (Blackwell Scientific, 1985).
6. K. C. Condie, *Chem. Geol.* **104**, 1–37 (1993).
7. C. J. Hawkesworth *et al.*, *J. Geol. Soc. London* **167**, 229–248 (2010).
8. B. Dhuime, A. Wuestefeld, C. J. Hawkesworth, *Nat. Geosci.* **8**, 552–555 (2015).
9. M. Tang, K. Chen, R. L. Rudnick, *Science* **351**, 372–375 (2016).
10. I. N. Bindeman, A. Bekker, O. D. Zakharov, *Earth Planet. Sci. Lett.* **437**, 101–113 (2016).
11. E. B. Watson, T. M. Harrison, *Science* **308**, 841–844 (2005).
12. J. W. Valley *et al.*, *Contrib. Mineral. Petrol.* **150**, 561–580 (2005).

13. M.-A. Millet *et al*., *Earth Planet. Sci. Lett.* **449**, 197–205 (2016).
14. N. D. Greber, N. Dauphas, I. S. Puchtel, B. A. Hofmann, N. Arndt, *Geochim. Cosmochim. Acta* **213**, 534–552 (2017).
15. K. J. Orians, E. A. Boyle, K. W. Bruland, *Nature* **348**, 322–325 (1990).
16. T. Taboada, A. M. Cortizas, C. García, E. García-Rodeja, *Geoderma* **131**, 218–236 (2006).
17. D. Garcia, M. Fonteilles, J. Moutte, *J. Geol.* **102**, 411–422 (1994).
18. Materials and methods and supplementary text are available as supplementary materials.
19. C. J. Allègre, D. Rousseau, *Earth Planet. Sci. Lett.* **67**, 19–34 (1984).
20. C. B. Keller, B. Schoene, *Nature* **485**, 490–493 (2012).
22. J.-F. Moyen, H. Martin, *Lithos* **148**, 312–336 (2012).
23. K. C. Condie, C. O'Neill, *Am. J. Sci.* **310**, 775–790 (2011).
24. N. Arndt, *J. Geophys. Res. Solid Earth* **108** (B6), 2293 (2003).
25. H. H. Dürr, M. Meybeck, S. H. Dürr, *Global Biogeochem. Cycles* **19**, 1–22 (2005).
26. R. L. Rudnick, S. X. Gao, in *Treatise on Geochemistry*, R. L. Rudnick, Ed. (Elsevier, 2003), pp. 1–64.
27. J. F. Moyen, G. Stevens, in *Archean Geodynamics Environments*, K. Benn, J.-C. Mareschal, K. C. Condie, Eds. (American Geophysical Union, 2006), pp. 149–175.
28. R. H. Smithies, *Earth Planet. Sci. Lett.* **182**, 115–125 (2000).
29. T. L. Carley *et al*., *Earth Planet. Sci. Lett.* **405**, 85–97 (2014).
30. E. Martin, H. Martin, O. Sigmarsson, *Terra Nova* **20**, 463–468 (2008).
31. S. P. Jakobsson, K. Jónasson, I. A. Sigurdsson, *Jokull* **58**, 117–138 (2008).
32. T. Tyrrell, *Nature* **400**, 525–531 (1999).
33. A. P. Gumsley *et al*., *Proc. Natl. Acad. Sci. U.S.A.* **114**, 1811–1816 (2017).

ACKNOWLEDGMENTS

This work was supported by grants from the Swiss National Science Foundation (grant P2BEP2_158983) to N.D.G.; NSF (grant CSEDI EAR1502591 and Petrology and Geochemistry grant EAR1444951) and NASA (grants LARS NNX17AE86G, EW NNX17AE87G, and SSW NNX15AJ25G) to N.D.; and NSF (grant EAR-05-45484), NASA (Astrobiology Institute Award NNA04CC09A), and the Natural Sciences and Engineering Research Council of Canada Discovery and Accelerator program to A.B. Comments on an earlier version of the manuscript by N. Arndt, M.-A. Millet, D. Rowley, R. Rudnick, and M. Tang are greatly appreciated. We also thank four reviewers for their constructive comments that improved the quality of the manuscript. We gratefully acknowledge N. Aubet, P. Fralick, G. Jackson, B. Krapež, A. Kuznetsov, A. Maslov, S. Master, P. Medvedev, T. Nägler, C. Noce, L. Ootes, F. Ossa-Ossa, E. Pecoits, T. Pettke, V. Podkovyrov, R. Rainbird, B. Rasmussen, R. Ruhanen, M.J. Severson, W. Su, D. Thomson, P. Thurston, and D. Winston for advice and access to sample collections. All data used in the paper are either tabulated in the supplementary material, published in the cited references, or archived in the PetDB Database (www.earthchem.org/petdb). N.D.G. and N.D. conceived the study. A.B., I.N.B., and A.H. selected and provided the samples. N.D.G. processed the samples and measured their Ti isotopic compositions. N.D.G., M.P.P., and N.D. compiled literature data and implemented the three-component mixing model. All authors contributed to writing and editing the manuscript.

SUPPLEMENTARY MATERIALS

www.sciencemag.org/content/357/6357/1271/suppl/DC1
Materials and Methods
Supplementary Text
Figs. S1 to S9
References (*34*–*98*)
Data Tables S1 to S10

25 May 2017; accepted 23 August 2017
10.1126/science.aan8086